Numerical Investigation of Switching of a Jet Generated by a Foil Pitching in Still Fluid

Chayanit Nigaltia and Sachin Y. Shinde

1 Introduction

Flying and swimming animals have motivated researchers to study flapping foils. Wings of aircraft and birds, propeller and helicopter rotor blades, tails of fish all have cross-sections of airfoil shape. For this reason, airfoil has remained a topic of immense interest for a long time.

How the natural flyers generate power for propulsion has been a topic of keen interest for researchers. Flapping foils have been studied extensively for the same. The phenomenon of thrust generation by a flapping foil in a fluid flow is known as Knoller–Betz effect. Jones et al. [1] experimentally and numerically investigated the Knoller–Betz effect on sinusoidally plunging airfoil. They reported that these unsteady thrust producing wakes are mainly due to inviscid phenomenon. Deflected wakes were also observed by them, leading to the production of lift and drag. Examination of the mean streamwise velocity field of a plunging NACA0012 airfoil in the absence of freestream velocity by Lai and Platzer [2] revealed that the velocity profiles were independent of the frequency of oscillation, when the jet velocity and the lateral distance were nondimensionalized by the peak plunge velocity and the amplitude of oscillation, respectively. Numerical viscous simulations by Lewin and Haj-Hariri [3] on a sinusoidally heaving symmetric airfoil, over a range of frequencies and amplitudes showed distinct solutions. Aperiodic and asymmetric solutions were also reported. Heathcote and Gursul [4] studied the jet switching phenomenon for a periodic plunging airfoil with varying stiffness in zero freestream velocity. The jet switching phenomenon was observed to be quasi-periodic. It was also observed that the switching frequency increases with increasing plunge frequency and plunge

C. Nigaltia (✉) · S. Y. Shinde
Indian Institute of Technology, Kanpur 175 005, India
e-mail: f1dr.chayanit@gmail.com

283

amplitude, and the amplitude of jet switching showed a decrease with decreasing Strouhal number ($St = fA/U_\infty$). Godoy-Diana et al. [5] experimentally studied the vortex wakes produced by a high aspect ratio flapping foil in a hydrodynamic tunnel. Transition from Benard-von Karman (BvK) to reverse Benard-von Karman (rBvK) and the symmetry breaking to asymmetric wakes was discussed. It was also observed that the transition from a BvK to rBvK wake precedes the actual drag-thrust transition. Godoy-Diana et al. [6] studied the vortex wakes, and the deflection angle of the mean jet is used to specify the asymmetry in the wake. A quantitative model based on the effective phase velocity ($U_P{}^*$), which is the velocity along the dipole direction induced by the vortex street, excluding the dipole velocity and the freestream velocity, to characterize the symmetry breaking was derived. Cleaver et al. [7] did an experimental investigation on plunging NACA0012 airfoil undergoing small amplitude and high-frequency oscillations with varying angle of attack (α). Bifurcations were observed at high St for the cases in which $\alpha \leq 10°$. Shinde and Arakeri [8] experimentally studied the flow produced by a rigid pitching airfoil in quiescent water. A weak jet was observed which changes direction continuously. This meandering was random and independent of initial conditions.

To study this switching phenomenon in great detail, the data has been captured for large number of cycles and at highly resolved time-steps. Acquiring this data experimentally is difficult, so numerical simulations have been performed.

The chapter is organized as follows: Sect. 2 presents the numerical formulation of the problem. Section 3 describes the jet switching pattern from a rigid pitching foil in still fluid. Some criteria are laid to classify the jet deflection as upward, downward or aligned along the centerline. The data obtained has been organized in a way to observe the switching process clearly at highly resolved time-steps. Finally, in Sect. 4, the conclusions are collected and the future scope of the research work has been discussed.

2 Numerical Formulation

2.1 Problem Statement and Flapping Kinematics

Simulations have been conducted to study the flow generated by an airfoil pitching in the absence of freestream velocity. We used open source software OpenFOAM 5.0 for simulations. NACA0015 airfoil has been considered for investigating the flow field. The motion profile is given as

$$\theta = \theta_{\max} \sin(2\pi f t) \tag{1}$$

where θ is the instantaneous pitching angle, $\theta_{\max}$ is the amplitude of oscillation, f is the pitching frequency and t is the time.
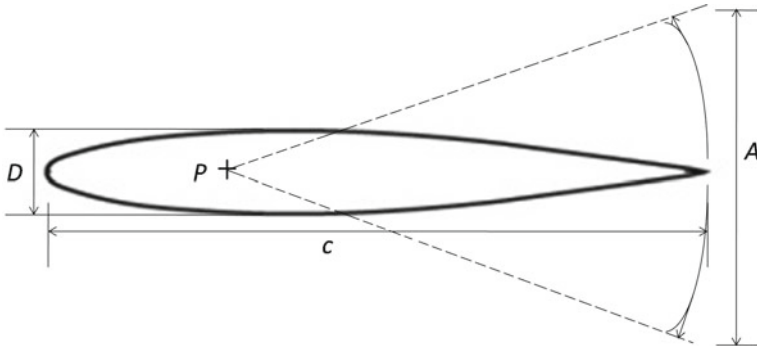
Fig. 1 Schematic diagram of a pitching foil

The peak-to-peak amplitude of the airfoil TE is denoted by A, chord by c, maximum airfoil thickness by D and the airfoil pitching point by P (Fig. 1).

The amplitude of oscillation (θ_{max}) and the pitching frequency (f) have been varied, keeping the mean angle of attack of the airfoil equal to zero and the flow has been studied. We studied four amplitudes ($\pm5°$, $\pm10°$, $\pm15°$ and $\pm20°$) and four frequencies (1, 2, 3 and 4 Hz) for each amplitude, thus constituting an all 16 cases.

2.2 Governing Equations and Discretization

Flow equations are solved using the arbitrary Lagrangian Eulerian (ALE) formulation on a mesh, which deforms with time. ALE form of incompressible Navier–Stokes equations is written as

$$\frac{\partial U}{\partial x} + \nabla.[(U - U_m)U] = -\nabla\left(\frac{p}{\rho}\right) + \upsilon\nabla^2 U \tag{2}$$

where ρ is the fluid density, U is the velocity of the fluid, U_m is the mesh velocity, p is the pressure and υ is the kinematic viscosity of the fluid.

Temporal discretization is first-order implicit Euler and a maximum Courant number (Co_{max}) of 0.8 is used to vary the corresponding time-step. The flux values are interpolated from cell centers to face centers linearly. Convective term is discretized using second-order upwinding and the diffusive term using central differencing.
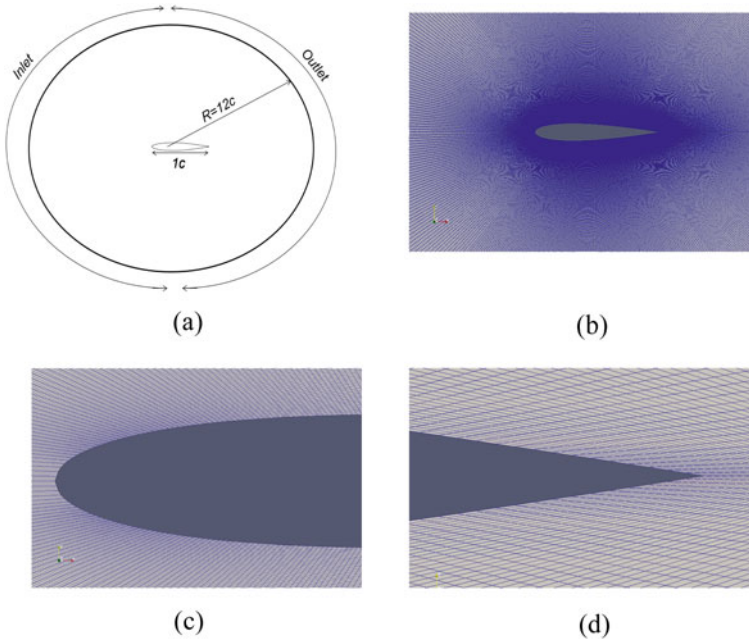
Fig. 2 **a** Computational domain, **b** grid around the airfoil, **c** closer view near LE, **d** closer view near TE

2.3 Computational Domain and Boundary Conditions

A schematic diagram of the computational domain is shown in Fig. 2. The domain is circular in shape with radius $12c$, where c is the chord length of the airfoil with center at the quarter-chord point, which is the pitch point of the airfoil. A circular region of radius $5c$ undergoes a pure pitching motion, while the outside grid remains stationary. The boundaries are far enough to eliminate boundary effects.

For velocity, a constant free stream boundary condition is kept at the inlet and a zero-gradient condition at the outlet boundary. On the airfoil, a moving wall boundary condition is imposed with no flux normal to the wall. A zero pressure gradient is kept at the inlet and on the airfoil, while a constant pressure condition is set at the outlet boundary.

2.4 Solver Details and Validation

Treatment of velocity equation is done using preconditioned bi-conjugate gradient (PBiCG) solver with diagonal incomplete-LU (DILU) preconditioner. The pressure equation has been handled using preconditioned conjugate gradient (PCG)

Fig. 3 Mean thrust coefficient (C_T) versus reduced frequency (k) plot of the airfoil with a pitching amplitude of $\theta_{max} = \pm 2°$. Data from the literature are included for comparison
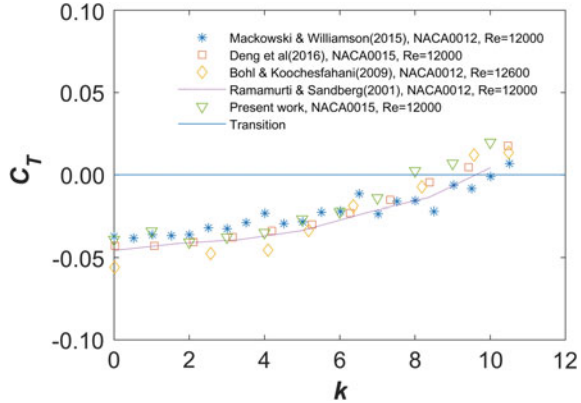
solver with diagonal incomplete-Cholesky (DIC) preconditioner. The velocity and the pressure equations are coupled using PISO algorithm.

The flow solver is validated quantitatively with the data from the literature. NACA0015 airfoil is used for validation with pitching point at quarter-chord distance from the LE. Figure 3 shows quantitative validation of the solver wherein the thrust coefficient (C_T) is plotted against the reduced frequency k defined as $k = (2\pi fc)/(2U_\infty)$. The plot shows good match with the previous studies. In comparison to the experimental study by Mackowski and Williamson [9] with NACA0012, for low and high k values, our C_D and C_T values are higher, respectively. This is due to the fact that NACA0015 being thicker than NACA0012 will produce larger drag force at low frequencies and at high frequencies will produce higher thrust. This fact is also reported by Jian Deng et al. [10]. The results have also been compared with the viscous simulations on NACA0012 by Ramamurti and Sandberg [11] and experimental results of Bohl and Koochesfahani [12].

A qualitative validation of the solver is also carried out by comparing the vorticity fields of the flow generated with the flow from Schnipper et al. [13] and Bohl and Koochesfahani [12]. We also performed a mesh independence study and observed that a mesh with 4,27,880 nodes gives satisfactory results. More details about the solver and validation can be found in Nigaltia's M.Tech thesis [14].

3 Results and Discussion

The results are discussed in detail for one case, namely $\theta_{max} = \pm 10°, f = 2$ Hz. The detailed features of the instantaneous and the time-averaged flow are presented, followed by discussion on the criterion used in the literature to detect and classify jet deflection. Later, our own criterion has been defined and described based on location of maximum resultant velocity magnitude. Further, a detailed investigation of the jet switching and meandering patterns is presented, and the jet switching is classified

into two patterns—abrupt and gradual. The temporal evolution of abrupt and gradual switching is studied in detail. Finally, the section is concluded by presenting a detailed and thorough investigation of the effect of variation in amplitude and frequency of pitching on the jet switching and meandering patterns.

3.1   The Flow

Figures 4 and 5 show the vorticity and velocity fields for three different instances, respectively, for the case $\theta_{max} = \pm 10°$ and $f = 2$ Hz, when the jet shows different deflection: downward, upward and along the centerline. In the absence of freestream velocity, there is no agency to convect the vortices away from the place of shedding. This is the main reason for the production of an inclined flow as commented by Shinde and Arakeri [8].

The time averaged flow is shown in Fig. 6. The averaged velocity and vorticity fields do not show the irregular patches as seen in the instantaneous flow fields. As will be evident later, the jet deflects and meanders randomly, which result in the
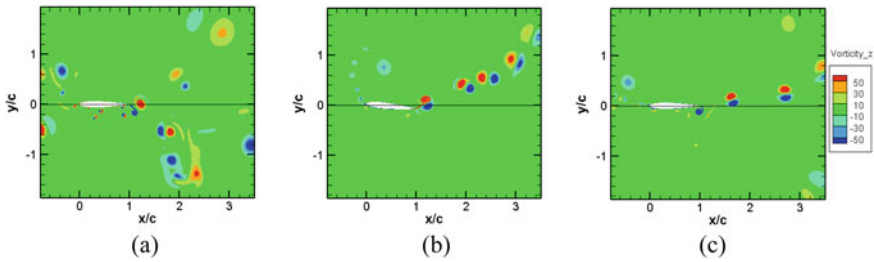
Fig. 4 Instantaneous spanwise vorticity contours at three different instances for the case $\theta_{max} = \pm 10°$ and $f = 2$ Hz, when the jet is **a** inclined in the downward direction, **b** inclined in the upward direction and **c** nearly along the centerline
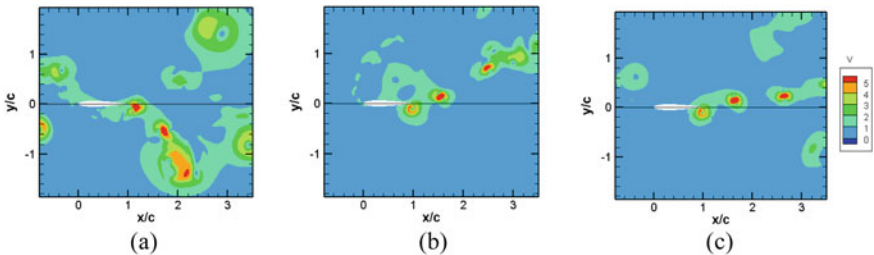
Fig. 5 Instantaneous resultant velocity contours at three different instances for the case $\theta_{max} = \pm 10°$ and $f = 2$ Hz, when the jet is **a** inclined in the downward direction, **b** inclined in the upward direction and **c** nearly along the centerline
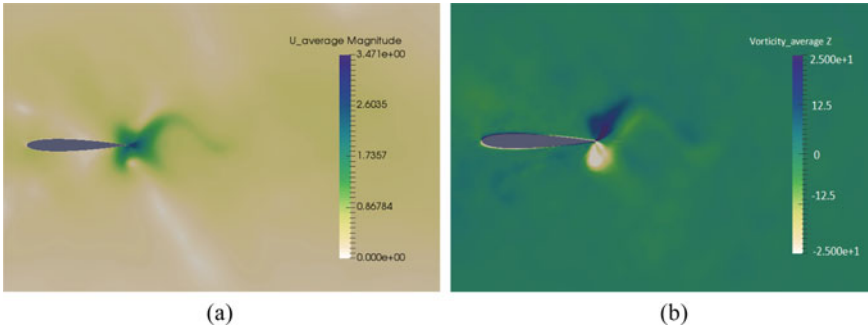
Fig. 6 Time averaged **a** resultant velocity and **b** spanwise vorticity field for the case $\theta_{max} = \pm 10°$ and $f = 2$ Hz

cancellation of the velocity and vorticity in the downstream over long time average. Some flow, however, is seen near the trailing edge region.

3.2 Criterion for Jet Deflection

Researchers have used different criteria to identify jet deflection. Heathcote and Gursul [4] while studying rigid and flexible foils observed the streamwise velocity distribution values at a point $(x/c, y/c) = (1, 0.5)$, where origin is assumed to be located at the airfoil TE. However, they did not present a clear picture of directionality of the jet. They observed quasi-periodicity in the variation of the streamwise velocity with time. Shinde and Arakeri[8] studied this switching phenomenon in pitching airfoil. They manually observed the jet flow field, and classified it into three different categories: upward (U), downward (D) and spread along centerline (S-C). The jet picks up directionality after some cycles and this direction keeps changing with time.

To identify and classify the jet deflection, maximum resultant velocities are plotted for all the time instants at five different sections $x/c = 0.5, 0.75, 1.0, 1.25, 1.5$ to look at the velocity variation over time, as shown in Fig. 7. It is decided to focus on two x-stations $x/c = 0.5$ and 1 as the deciding criteria for jet deflection. In case, it is difficult to decide based on the two sections, one more x-station at $x/c = 1.25$ is considered.

3.3 Jet Inclination

To get the idea of the switching pattern of the generated jet, interrogation points are set at $y/c = \pm 0.25$, at different x/c sections, after looking at the velocity and the vorticity fields. If the maximum resultant velocity locations are present beyond these
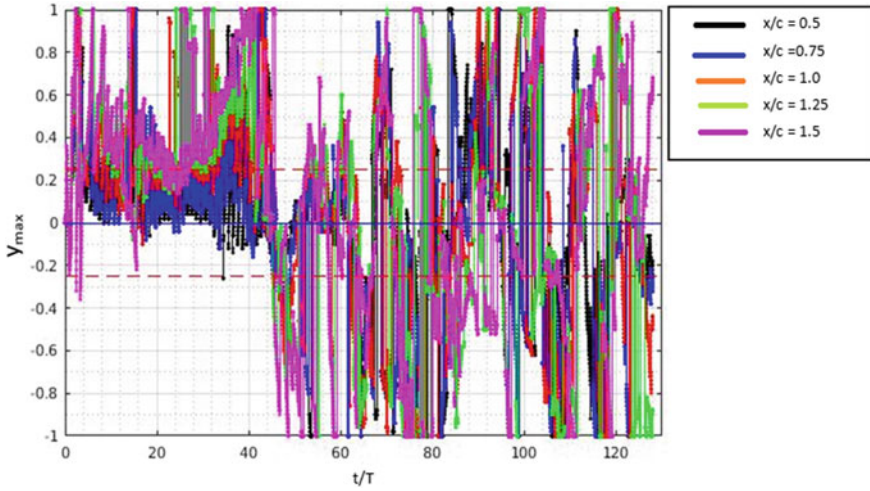
Fig. 7 Plots showing location of maximum resultant velocity at every instant at different streamwise × locations, for $\theta_{max} = \pm10°$ and $f = 2$ Hz

y-locations, then this may be because of stray vortices present in the flow, and hence we neglect it. Let the numbers 1, 2 and 3 denote the sections at $x/c = 0.5$, 1 and 1.25, respectively, so $y1_{max}$ will give the transverse location of maximum resultant velocity at Sect. 1 at a particular instant.

Using the criteria detailed in Table 1, the jet inclination data is obtained for the case when $\theta_{max} = \pm10°$ and $f = 2$ Hz, for 128 cycles (Fig. 8). The jet switches direction randomly, as observed from the figure, and the switching is sometimes abrupt and sometimes gradual. It is evident from Fig. 8 that the jet stays in one particular orientation for a time period which ranges from a fraction of a cycle to several cycles, and also it keeps changing the direction continuously and randomly.

	$y1_{max}$	$y2_{max}$	$y3_{max}$	Deflection
Table 1 Criteria used for classifying jet deflection. $y1$, $y2$, $y3$ represent the y-location of maximum resultant velocity at three x-stations, respectively, at $x/c = 0.5$, 1 and 1.25	>0.25	>0.25	–	Upward (U)
	0< , <0.25	>0.25	–	Upward (U)
	>0.25	0< , <0.25	>0.25	Upward (U)
	>0.25	0< , <0.25	<0.25	Center (C)
	<−0.25	<−0.25	–	Downward (D)
	0> , >−0.25	<−0.25	–	Downward (D)
	<−0.25	0> , >−0.25	<−0.25	Downward (D)
	<−0.25	0> , >−0.25	>−0.25	Center (C)
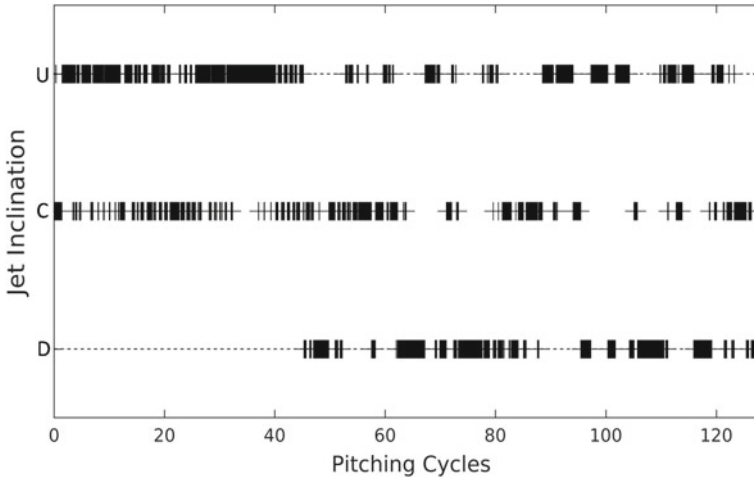
Fig. 8 Jet inclination data for the case when $\theta_{max} = \pm 10°$ and $f = 2$ Hz. The figure shows random switching. U, D, C, respectively, indicate upward, downward deflected jet and jet along the centerline

3.4 Temporal Evolution of the Switching Process

By looking at the jet inclination (Fig. 8) and the maximum velocity transverse location plot (Fig. 9), it is observed that the jet sometimes changes direction abruptly and sometimes gradually. Cycle time at section $x/c = 0.5$ is extracted to observe these switching patterns.

From the maximum velocity transverse location plot, it can be seen that gradual switching is taking place for 3 cycles, from 60 to 63 cycles and the sudden switching happens several times between 35 and 40 cycles. Figure 9 shows the zoomed view of the cycle period of interest and the jet inclination data in case of gradual switching. Similarly, Fig. 10 shows the zoomed view of the cycle period of interest and the jet inclination data in case of sudden switching. Sudden switching indicates that the time scale of switching is even smaller than the smaller time scale used in the simulations, that is, $t/T = 0.01$ and it needs further investigation with a time-step much smaller than that used in present simulations.

3.5 Parametric Study

A similar kind of study has been carried out by varying four amplitudes ($\theta_{max} = \pm 5°, \pm 10°, \pm 15°$ and $\pm 20°$) and four frequencies ($f = 1, 2, 3$ and 4 Hz), for each amplitude. We observed a deflected jet that continually and randomly changes the directions in all the 16 cases studied. We present the data for two representative
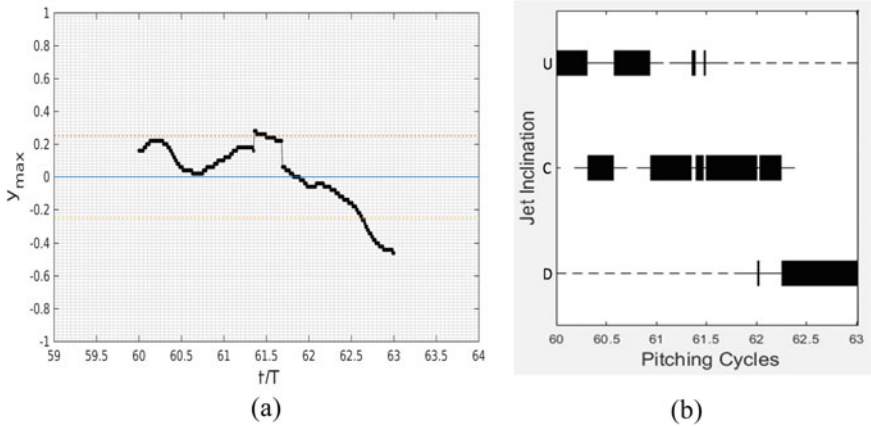
Fig. 9 Figure showing **a** gradual switching and **b** jet inclination data for the case $\theta_{max} = \pm 10°$ and $f = 2$ Hz
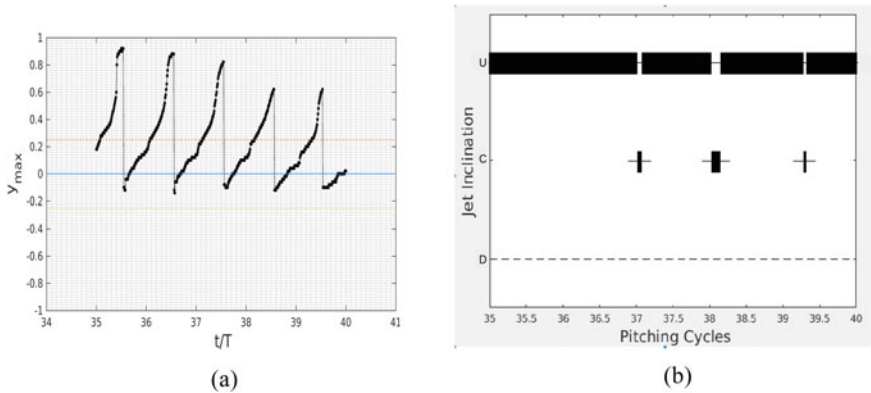

Fig. 10 Figure showing **a** sudden switching and **b** jet inclination data for the case $\theta_{max} = \pm 10°$ and $f = 2$ Hz

cases corresponding to $\theta_{max} = \pm 15°, f = 1$ Hz and $\theta_{max} = \pm 20°, f = 3$ Hz. The jet inclination plot is shown in Fig. 11. It appears that amplitude and frequency does not have any particular effect on the jet switching pattern.

4   Conclusions and Future Scope

The flow generated by a symmetric NACA0015 foil pitching about quarter-chord point from the leading edge in the absence of freestream velocity is studied. The flow is studied by varying amplitude and frequency of pitching. The present work is
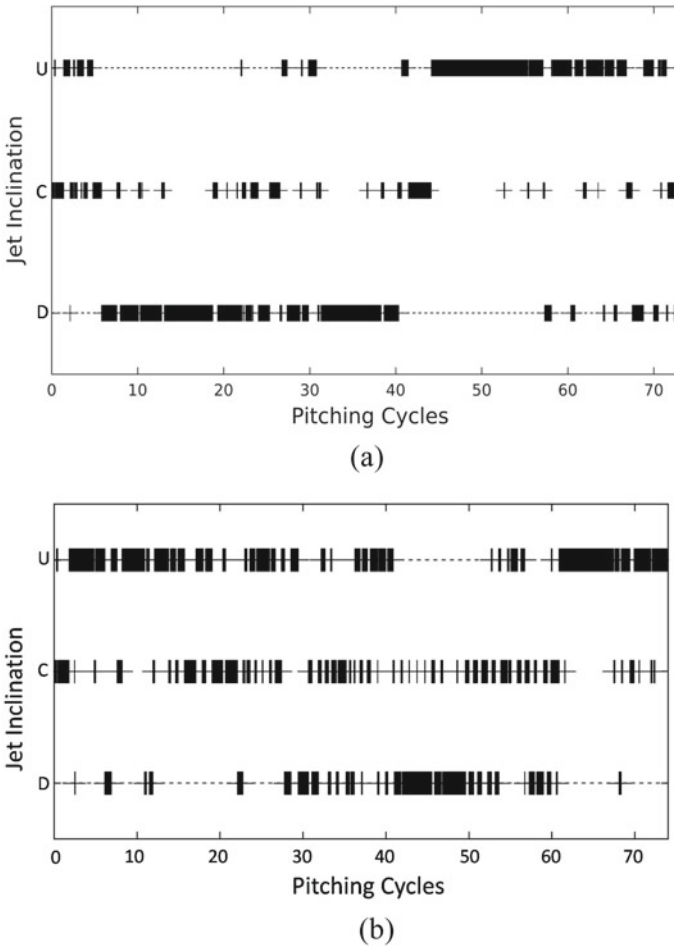
Fig. 11 Jet inclination data for the case for **a** $\theta_{max} = \pm 15°, f = 1$ Hz and **b** $\theta_{max} = \pm 20°, f = 3$ Hz

aimed to explore the jet deflection and meandering trends generated by a foil pitching in an otherwise still fluid. To identify and classify the jet deflection, a criterion is designed based on the y-location of the maximum resultant velocity at two or three x-stations located at $x/c = 0.5, 1, 1.25$. It was observed that the jet remains in one particular orientation for time periods which range from some fraction of a cycle to several cycles and the jet changes the inclination continuously and randomly. No pattern, quasi-, or periodicity in the jet switching pattern was observed. Two types of switching process—gradual and sudden—were observed. The time resolution used in the simulations was found to be insufficient, to study sudden switching. The parametric study conducted by varying amplitude and frequency of pitching reveals

that amplitude and frequency do not have any particular effect on switching pattern, and the switching is observed to be random in all the cases.

The controlled jet deflection from flapping foils can be exploited in man-made devices for turning and maneuvering activities. If by any regulated process, this jet deflection can be eliminated, the straight jet can be used for straight line propulsive motions. Both these things, the straight and the deflected jets can be utilized efficiently by the humans and can pave the way of building the artificial propellers. The artificial propellers may be more efficient than the conventionally used propellers. Flow investigation for even longer time may reveal some different jet switching pattern. Hence, the flow demands further investigation for longer duration. In case of abrupt switching, the simulations need to be carried out at even smaller time-steps, which can reveal very interesting details on switching patterns. The criterion used to classify the jet inclination seems to be less robust for some instances when the stray vortices arrive at the investigation stations.

References

1. Jones, K.D., Dohring, C.M., Platzer, M.F.: Experimental and computational investigation of the Knoller-Betz effect. AIAA J. **36**, 1240 (1998)
2. Lai, J.C.S., Platzer, M.F.: Characteristics of a plunging airfoil at zero freestream velocity. AIAA J. **39**, 531 (2001)
3. Lewin, G.C., Haj-Hariri, H.: Modelling thrust generation of a two-dimensional heaving airfoil in a viscous flow. J. Fluid Mech. **492**, 339 (2003)
4. Heathcote, S., Gursul, I.: Jet switching phenomenon for a periodically plunging airfoil. Phys. Fluids **19**, 027104 (2007)
5. Godoy-Diana, R., Aider, J., Wesfreid, J.E.: Transition in the wake of a flapping foil. Phys. Rev. E **77**, 016308 (2008)
6. Godoy-Diana, R., Marais, C., Aider, J., Wesfreid, J.E.: A model for the symmetry breaking of the reverse B´enard–von K´arm´an vortex street produced by a flapping foil. J. Fluid Mech. **622**, 23 (2009)
7. Cleaver, D.J., Wang, Z., Gursul, I.: Bifurcating flows of plunging aerofoils at high Strouhal numbers. J. Fluid Mech. **708**, 349 (2012)
8. Shinde, S.Y., Arakeri, J.H.: Jet meandering by a foil pitching in quiescent fluid. Phys. Fluids **25**, 041701 (2013)
9. Mackowski, A., Williamson, C.: Direct measurement of thrust and efficiency of an airfoil undergoing pure pitching. J. Fluid Mech. **765**, 524–543 (2015)
10. Deng, J., Sun, L., Teng, L., Pan, D., Shao, X.: The correlation between wake transition and propulsive efficiency of a flapping foil: a numerical study. Phys. Fluids **28**, 094101 (2016)
11. Ramamurti, R., Sandberg, W.: Simulation of flow about flapping airfoils using finite element incompressible flow solver. AIAA J. **39**, 253–260 (2001)
12. Bohl, D.G., Koochesfahani, M.M.: MTV measurements of the vortical field in the wake of an airfoil oscillating at high reduced frequency. J. Fluid Mech. **620**, 63 (2009)
13. Teis, S., Andersen, C.A., Bohr, T.: Vortex wakes of a flapping foil. J. Fluid Mech. **633**, 23 (2009).
14. Nigaltia, C.: Numerical investigation of switching of a jet generated by a foil pitching in still fluid. M.Tech thesis (Indian Institute of Technology, Department of Mechanical Engineering, India, 2019).